DOI 10.1007/s11182-021-02256-y
Russian Physics Journal, Vol. 63, No. 11, March, 2021 (Russian Original No. 11, November, 2020)

STUDY OF THE OPTICAL ATMOSPHERIC DISTORTIONS USING WAVEFRONT SENSOR DATA

P. G. Kovadlo,[1] A. Yu. Shikhovtsev,[1] E. A. Kopylov,[2,3] A. V. Kiselev,[1] and I. V. Russkikh[1]

UDC 551.5

The paper studies the optical turbulence structure at the Large Solar Vacuum Telescope of the Baikal Astrophysical Observatory. Some results on the study of the wavefront distortions are given to expand the data archive. The possibilities of detecting layers with enhanced optical turbulence intensity in the atmosphere are discussed. The altitudes of the atmospheric turbulent layers within the boundary layer are estimated.

Keywords: telescope, wavefront, Fried's radius, turbulence.

INTRODUCTION

Atmospheric turbulence significantly decreases the resolution of ground-based telescopes and limits the isoplanatic angle of the atmosphere. The value that characterizes the turbulence strength is the structural characteristic of air refractive index fluctuations entering into the 2/3 Kolmogorov–Obukhov law. The Fried radius [1] is conventionally used as an integral characteristic of the optical turbulence strength along the line of sight.

To achieve a maximum resolution in the preset field of view, the astronomical ground-based telescopes already operating or planned for commissioning [2] are equipped with adaptive optics systems of different designs. The efficiency of image correction aimed at an increase in the spatial resolution using the adaptive optics system depend on the optical turbulence characteristics along the line of sight and, in particular, on the average values and variances of the Fried radius. The optimal choice of the technical parameters of the adaptive optical system is performed taking into account the optical scheme of the telescope and the special features of the vertical profiles of the structural characteristics of air refractive index fluctuations together with the vertical wind velocity profiles. In this case, the vertical profiles of the meteorological parameters change significantly both for short and long time intervals. From this viewpoint, the estimation of the Fried radius as the characteristic of the rugged wavefront and of the vertical profiles of the meteorological parameters is of interest for astroclimatic research of the measurement site and optimization of the appearance and technical characteristics of the adaptive optics system.

[1]Institute of Solar-Terrestrial Physics of the Siberian Branch of the Russian Academy of Sciences, Irkutsk, Russia, e-mail: kovadlo2006@rambler.ru; Ashikhovtsev@iszf.irk.ru; kiselev@iszf.irk.ru; vanekrus@iszf.irk.ru; [2]Institute on Laser and Information Technologies – Branch of the Federal Scientific Research Center "Crystallography and Photonics" of the Russian Academy of Sciences, Shatura, Moscow Region, Russia; [3]V. E. Zuev Institute of Atmospheric Optics of the Siberian Branch of the Russian Academy of Sciences, Tomsk, Russia, e-mail: kea@iao.ru.
Translated from Izvestiya Vysshikh Uchebnykh Zavedenii, Fizika, No. 11, pp. 109–114, November, 2020. Original article submitted November 15, 2019; revision submitted July 31, 2020.

TABLE 1. Fried's Radius Calculated from Measurements on June 28, 2018.

Time	14.39	14.41	14.42	14.44	14.46	14.50	14.51	14.52
r_0, cm	5.81	4.96	5.03	4.11	3.83	4.80	3.87	6.38

ESTIMATION OF THE FRIED RADIUS FROM MEASUREMENTS WITH THE WAVEFRONT SENSOR. S-DIMM+ METHOD OF DETERMINING THE VERTICAL PROFILES OF THE OPTICAL TURBULENCE

To expand the archive of data on the structure of the optical turbulence and on the wavefront distortion characteristics at the site of the Large Solar Vacuum Telescope (LSVT), long-term optical and micrometeorological measurements have been carried out. By means of the BSVT wavefront sensor, the Hartmann images – sets of spaced subimages of the same object on the solar surface (pores, spots, or edge fragments) – are recorded and archieved. The methods of measuring and studying of the optical distortions formed along the line of sight of the adaptive systems [3] are being improved. Mast measurements of the turbulence characteristics in the surface layer up to altitudes of ~30 m above the underlying surface, including synchronous with optical measurements, are practically continuously carried out. Results of investigation of the structure of optical and micrometeorological turbulence are presented in [4–10].

In this work, the process of forming wavefront distortions is studied based on an analysis of the differential image jitters measured with the Shack–Hartmann LSVT wavefront sensor performed in 2018. The values of the Fried radius estimated from these measurements were described in detail in [6]. Table 1 presents values of the Fried radius estimated from measurements of the differential jitter of images on June 28, 2018.

The obtained values of the Fried radius give an idea of changes of the total optical turbulence energy along the LSVT line of sight and provide the basis for an analysis of the physical pattern of forming the wavefront distortions. At the same time, in addition to the analysis of the integral characteristics of the optical turbulence, its structure in different attitude layers can be studied using the triangular method of analysis of small-scale wavefront distortions. Among the methods and their modifications, the Slodar and S-DIMM+ methods based on recording and ranging of small-scale wavefront distortions are widely used [10–15].

The essence of the S-DIMM+ method of determining the vertical profiles of the optical turbulence from the data of measurements with the Shack–Hartmann sensor were described in detail in [10] together with restrictions on its applications. The method is based on the relationship between the cross-correlation function of differential displacement of the centers of gravity of subimages and the vertical distribution of the energy characteristic of turbulent air refractive index fluctuations. The displacements of the subimage centers of gravity along the mutually perpendicular coordinate axes are proportional to the total contribution of different atmospheric layers:

$$C_{sx} =< \delta x_1(s,0)\delta x_2(s,\alpha) >= \sum_{n=1}^{N} c_n F_x(s,\alpha,h_n), \quad (1)$$

$$C_{sy} =< \delta y_1(s,0)\delta y(s,\alpha)_2 >= \sum_{n=1}^{N} c_n F_y(s,\alpha,h_n), \quad (2)$$

where s is the distance from the reference subaperture, α is the angle between the *axial* and *off-axis* objects, and h_n is the altitude of the *n*th turbulent layer. The differential displacements of the axial ($\alpha = 0$) and off-axis ($\alpha \neq 0$) objects are defined as follows:

$$\delta x_1(s,0) = \sum_{n=1}^{N} x_n(s) - x_n(0), \quad (3)$$

$$\delta x_2(s,\alpha) = \sum_{n=1}^{N} x_n(s + \alpha h_N) - x_n(\alpha h_N) . \quad (4)$$

The functions $F_x(s,\alpha,h_n)$ and $F_y(s,\alpha,h_n)$ were presented in [10]. The coefficients c_n are proportional to the optical turbulence intensity in the atmospheric layer:

$$c_n = 5.98 D_{\text{eff}}(h_n)^{-1/3} C_n^2 dh / \cos z . \quad (5)$$

Since the expressions for the differential displacements along the *y* axis have analogous form, to reveal the special features in the vertical structure of the optical turbulence, below we analyze the displacements only along one axis.

The S-DIMM+ method implements the approach to accumulation of the data on the turbulence structure from the image of the refraction pattern described in monograph [16]. In particular, considering the approach in a broad sense, it is possible to consider that if the turbulence distributed in a turbulent zone is homogeneous and if the turbulence scale is very small compared to the cross section of this zone, the distribution pattern of the optical distortions in the aperture plane should be equivalent to that of the turbulence distribution in the longitudinal cross section of this zone. Within the limits of the S-DIMM+ method, the pattern of the turbulence distribution along the line of sight was estimated from measurements of the differential displacement of the spaced sub-image fragments that minimizes the instrumental distortions due to the wind flow around the telescope.

SPATIAL CROSS-CORRELATION FUNCTIONS OF THE JITTER OF IMAGES AT THE LARGE SOLAR VACUUM TELESCOPE

When solving problems of solar image correction, attention is focused at the study of the wavefront within the wide field of view. We take advantage of one of the well-known approaches to the determination of the wavefront distortions at different altitudes consisting in the triangulation of local wavefront tilts measured by the Shack–Hartmann sensor. In spite of the fact that the vertical profiles of the optical turbulence based on an analysis of small-scale wavefront distortions are reconstructed on average to altitudes of 3–5 km [13, 17], the adaptive optics characteristics are significantly influenced exactly by the atmospheric boundary layer.

To determine the wavefront distortions and the contribution of atmospheric turbulence layers to the distortions of the measurement data, the Shack–Hartmann sensor put in the optical LSVT scheme was used. As a light source, the image of an edge of the solar disk was used the analysis of which allowed the displacements of separate fragments of the image spaced at different angles to be determined. In wavefront measurements, the field of view of each subaperture was 38 sec of arc.

The subimages of the solar disk edge are the spatial light sources providing the possibility of analyzing separate subimage fragments. Each subimage in the focal plane of the subaperture was subdivided into separate fragments separated from each other approximately by 1 sec of arc within the field of view equal to 38 sec of arc. For each fragment of the subimage of the solar disk edge, the time series of changes of the positions of the center of gravity was determined. Thus, 38 time series of changes of the spatial positions of the center of gravity of the subimage fragments were obtained.

From formula (1), we calculated the spatial cross-correlation functions of the image jitter for different subapertures spaced at distances of 7.5 cm (Fig. 1), 15 cm (Fig. 2), 30 cm (Fig. 3) and 52.5 cm (Fig. 4). The curves in these figures show the spatial cross-correlation functions for these subaperture pairs.

With increase in the active part of the telescope diameter, the maximum of the spatial cross-correlation functions of the jitter of images should be displaced towards larger angles between the light "sources" – the chosen fragments of the subimages of the solar edge. This displacement can be seen in Figs. 1–4. In the adjacent subapertures, when δi = 1, the maximum of the function is observed at angles from 6.0 to 7.5 sec of arc. With increase in the active part of the telescope diameter, it is displaced by 12–15 sec of arc for the subaperture centers spaced at 15 cm, by ~24.0–28.0 sec of arc for 30 cm spacing, and then displaced beyond the scale.

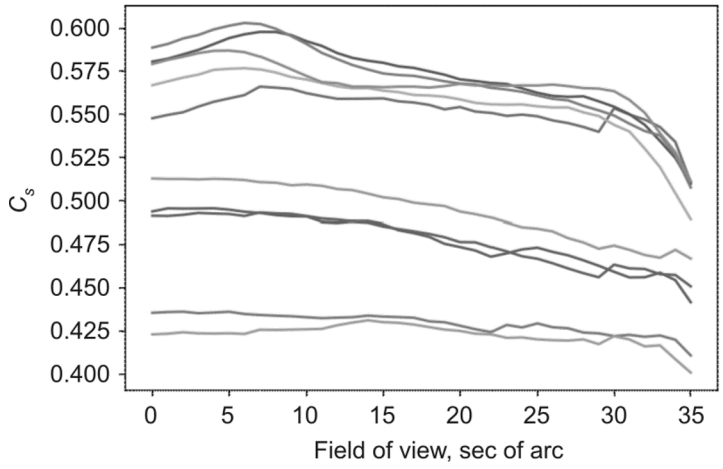

Fig. 1. Spatial cross-correlation functions of the jitter of images spaced at a minimal distance of 7.5 cm. Measurements at the Large Solar Vacuum Telescope on June 28, 2018 at 14:41, local time.

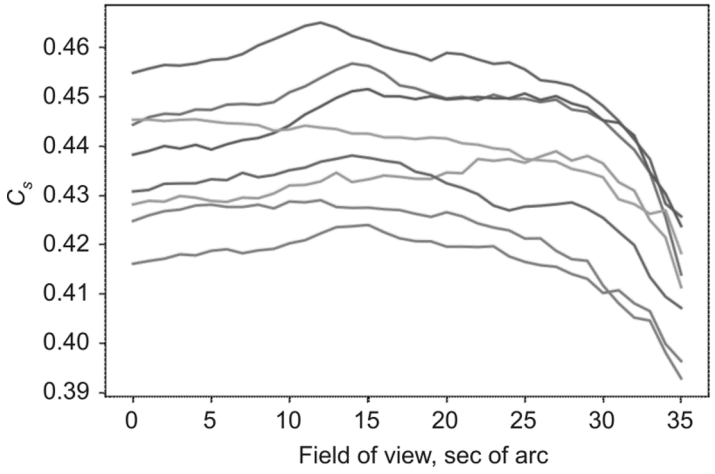

Fig. 2. Spatial cross-correlation functions of the jitter of images spaced at 15 cm. Measurements at the Large Solar Vacuum Telescope on June 28, 2018, at 14:41, local time.

To estimate the profiles of the dimensionless turbulence characteristic $C_{\text{norm}} = c_n / A$, the spatial cross-correlation functions should be normalized by the correlation function A of the reference subaperture used in [18]. Figure 5 shows the changes of the dimensionless turbulence characteristic C_{norm} across the field of view. At large angles affected by the lower-lying turbulence layers, C_{norm} exceeded its values observed at small angles.

DISCUSSION OF RESULTS

From the jitter of subimages measured with the Shack–Hartmann sensor, we estimated the displacements of positions of the centers of gravity in the spatial cross-correlation functions. By the method of triangulation of wavefront distortions, we determined the altitudes of the atmospheric turbulent layers proportional to the angular displacement

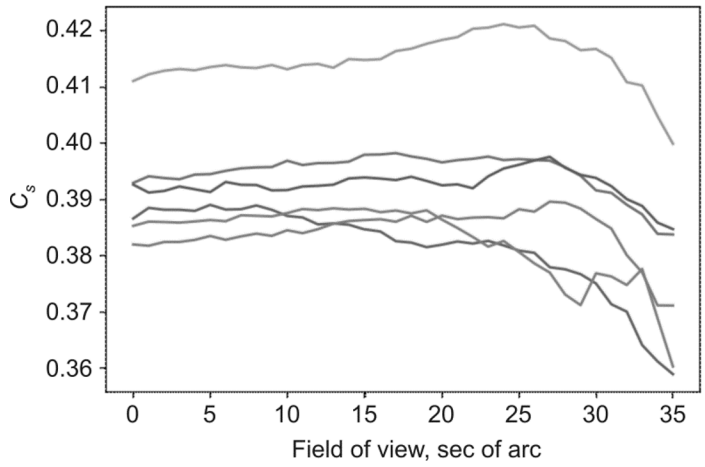

Fig. 3. Spatial cross-correlation functions of the jitter of images spaced at 30 cm. Measurements at the Large Solar Vacuum Telescope on June 28, 2018, at14:41, local time.

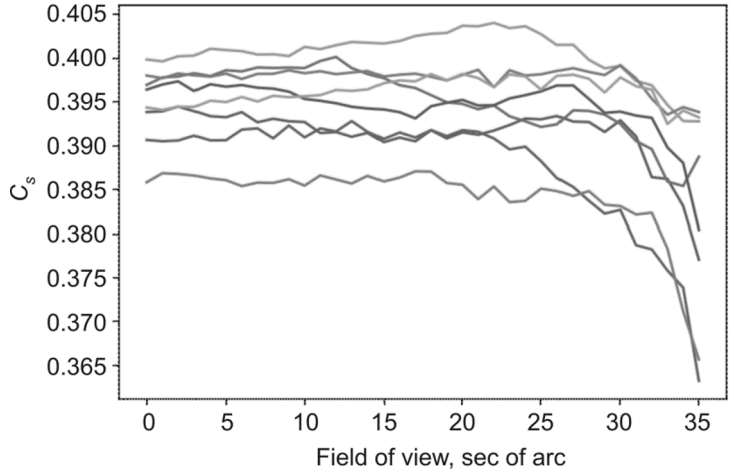

Fig. 4. Spatial cross-correlation functions of the jitter of images spaced at 52.5 cm. Measurements at the Large Solar Vacuum Telescope on June 28, 2018, at 14:41, local time.

between the fragments of solar edge subimages. The results are generalized in Table 2. The first column presents the distance between the centers of the two chosen subapertures, the second column gives the angle between the two fragments of the edge image spaced at a fixed angle within the subaperture, the third column gives the altitude of the atmospheric turbulent layer which distorts the spatial cross-correlation functions. In the fourth column, the character of the spatial cross-correlation functions is indicated. It follows that at the Large Solar Vacuum Telescope, the turbulent layers were observed at altitudes of 1150–1440 m and 570–640 m. This is in agreement with the typical atmospheric layer altitudes [19].

The data on the spatial cross-correlation functions of the jitter of images of spaced sources can further be used for calculation of the vertical profiles of the optical turbulence intensity, for example, the structural characteristic of the air refractive index fluctuations in real time. The methods of reconstruction of the vertical profiles of the structural characteristic of air refractive index fluctuations along the line of sight with application of remote methods based on

TABLE 2. Altitudes of the Atmospheric Turbulent Layers Determined from the Maxima (Peaks) of the Spatial Cross-Correlation Functions of the Jitter of Fragments of the LSVT Subimages of the Solar Edge

D/n, cm	θ, sec. of arc	z, m	Character of changes of the *Cs* value
7.5 ($\delta i = 1$, $\delta j = 1$)	~6.0–7.5	~1150–1430	Mild peak
15($\delta i = 2$, $\delta j = 2$)	~12.0–15.0	~1150–1440	Mild peak
15($\delta i = 2$, $\delta j = 2$)	~27.0–30.0	~570–640	Mild peak
30 ($\delta i = 4$, $\delta j = 4$)	~24.0–28.0	~1230–1430	Mild peak
52.5 ($\delta i = 7$, $\delta j = 7$)	~22.0–35.0	~1480–2350	Weak growth of the *Cs* value

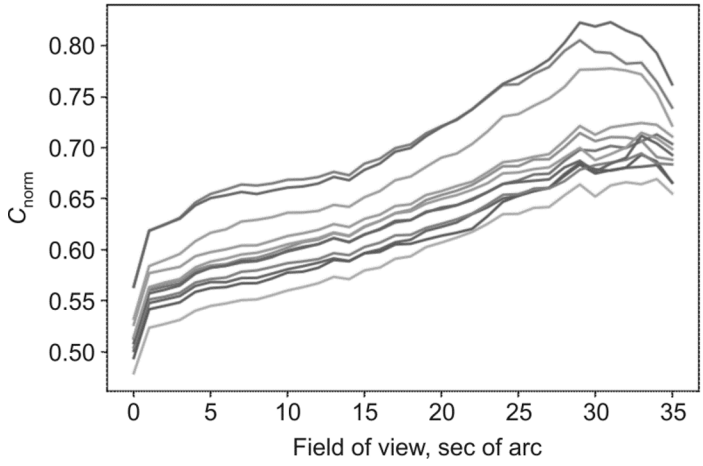

Fig. 5. Changes of the dimensionless turbulence characteristic C_{norm} across the field of view. The increase in the field of view corresponds to the decrease of the turbulent layer altitude. Measurements at the Large Solar Vacuum Telescope on june 28, 2018, at 14:41, local time.

measurements with the wavefront sensors can be implemented in the adaptive optical system with expanded field of view of the KST-3 Large Solar Telescope.

The reconstruction of the turbulent characteristics by the S-DIMM+ method was supported by the Agreement No. 075-15-2019-628, and the analysis of the altitude distribution of the turbulence was supported by the Russian Science Foundation (Grant No. 19-79-00061). The measurement data were partly obtained using the Unique Scientific Installation – the Large Solar Vacuum Telescope – within the framework of Project II.16 of the Fundamental Scientific Research Program.

REFERENCES

1. D. L. Fried, J. Opt. Soc. Am., **55**, 1427–1435 (1965).
2. V. M. Grigoriev, M. L. Demidov, D. Yu. Kolobov, *et al*., Solar-Terr. Phys., **6**, No. 2, 19–36 (2020).
3. V. P. Lukin, L. V. Antoshkin, L. A. Bolbasova, *et al*., Atmospheric Ocean. Optics, **33**, No. 1, 85–103 (2020).
4. P. G. Kovadlo, P. A. Naydenov, and A. Yu. Shihovzev, The Bull. Irkutsk State Univ. Ser. "Earth Sci.," **2**, No. 2, 105–116 (2009).
5. N. N. Botygina, P. G. Kovadlo, E. A. Kopylov, *et al*., in: International Baikal Youth Scientific School in Fundamental Physics BSFF-13, Irkutsk (2013), pp. 303–305.
6. N. N. Botygina, E. A. Kopylov, V. P. Lukin, *et al*., Atmospheric Ocean. Optics, **27**, No. 2, 142–146 (2014).

7. E. A. Kopylov, A. A. Selin, and A. Yu. Shihovzev, Izv. Vyssh. Uchebn. Zaved., Fiz., **58**, No. 10/3, 104–106 (2015).
8. P. A. Konyaev, E. A. Kopylov, V. P. Lukin, *et al*., Proc. SPIE, **10466**, 104660N (2017).
9. L. A. Bolbasova, A. Yu. Shikhovtsev, V. P. Lukin, and P. G. Kovadlo, MNRAS, **482**, 2619–2626 (2019).
10. M. Tham, Wide field wavefront sensing: Undergraduate Thesis in Astronomy, Department of Astronomy, Stockholm University, Stockholm (2011).
11. G. B. Scharmer and T. I. van Werkhoven, A&A, **513**, A25 (2010).
12. A. Yu. Shikhovtsev, A. V. Kiselev, P. G. Kovadlo, *et al*., Opt. Atm. Okeana, **32**, No. 12, 994–1000 (2019).
13. A. Yu. Shikhovtsev, P. G. Kovadlo, L. A. Bolbasova, and V. P. Lukin, Opt. Atm. Okeana, **32**, No. 10, 819–823 (2019).
14. V. V. Nosov, V. P. Lukin, E. A. Nosov, and A. V. Torgaev, Izv. Vyssh. Uchebn. Zaved. Fiz., **59**, No. 12/2, 138–142 (2016).
15. A. Yu. Shikhovtsev, A. V. Kiselev, P. G. Kovadlo, *et al*., Atmospheric Ocean. Optics, **33**, No. 3, 295–301 (2020).
16. J. O. Hintze, Turbulence [Russian translation], GIFML, Moscow (1963).
17. A. Shikhovtsev, P. Kovadlo, V. Lukin, *et al*., Atmosphere, **10**, No. 11, 661 (2019).
18. A. Yu. Shikhovtsev, A. V. Kiselev, P G. Kovadlo, and I. V. Russkikh, in: Works of the International Baikal Youth Scientific School in Fundamental Physics BSFF-2019, Irkutsk (2019), pp. 402–404.
19. V. A. Banakh, I. N. Smalikho, and A. V. Falits, Remote Sensing, **12**, No. 6, 955 (2020).